Generation and detection of nonclassical field states by conditional measurements following two-photon resonant interactions

B. M. Garraway,[1] B. Sherman,[2] H. Moya-Cessa,[1,*] P. L. Knight,[1] and G. Kurizki[2]
[1]*Optics Section, The Blackett Laboratory, Imperial College, London SW7 2BZ, United Kingdom*
[2]*Department of Chemical Physics, Weizmann Institute of Science, Rehovot 76100, Israel*
(Received 19 January 1993)

A simple scheme is presented that allows the generation and detection of nonclassical states of the electromagnetic (em) field with controllable (predetermined) photon-number and phase distributions. It is based on the two-photon resonant interaction of a single em field mode in a high-Q cavity with initially excited atoms crossing the cavity sequentially (one at a time). The sequence duration should be much shorter than the cavity-mode lifetime. Nonclassical states of the field are generated conditionally, by selecting only those sequences wherein each atom is measured to be in the excited state after the interaction. The field distribution resulting from a sequence of N such measurements is peaked about $2N$ positions in the phase plane, which evolve sinusoidally as a function of the atomic transit times and are therefore simply controlled. When these peaks are chosen not to overlap, the field state constitutes a generalized Schrödinger cat. By choosing them to overlap, we can make parts of the field distribution strongly interfere, giving rise to decimation of the photon-number distribution. In particular, this process can prepare Fock states with controlled photon numbers. The generated phase distribution can be detected by monitoring the pattern of revivals in the excitation of a "probe" atom.

PACS number(s): 42.50.−p, 42.52.+x

I. INTRODUCTION

A major effort has been directed towards the generation of nonclassical states of the electromagnetic (em) field, in which certain observables exhibit less fluctuations (or noise) than in a coherent state, whose noise is referred to as the standard quantum limit (SQL). Nonclassical states that have attracted the greatest interest in recent years include (a) macroscopic quantum superpositions (MQS) of quasiclassical coherent states with different mean phases or amplitudes, nicknamed "Schrödinger cats" [1–3], (b) squeezed states [4,5], whose fluctuations in one of the quadratures or the amplitude are reduced below the SQL, and (c) the particularly important limit of extreme amplitude squeezing, namely, Fock (photon-number) states [6].

The interaction of one atom (at a time) with a single mode of a high-Q cavity yields a variety of spectacular nonclassical field effects, among them sub-Poissonian photon statistics (intensity noise reduction below the SQL) that have been demonstrated experimentally [7]. By contrast, neither Schrödinger cats nor Fock states have been observed as yet. Most theoretical schemes that have been suggested for the realization of these "fragile" states are based on the fundamental Jaynes-Cummings model (JCM), which pertains to a two-level atom, interacting with a single quantized field mode [8–12]. This class of schemes includes (a) generation of Schrödinger cats by many atoms initially prepared (by a $\pi/2$ pulse) in a polarized state whose sequential transit through the cavity gradually builds up an approximate trapping state of the field, described by a superposition of the vacuum and a number state [12]; (b) generation of a Schrödinger cat with a π phase difference, via the remarkable disentanglement of the atomic and field states, for an atomic transit time that is exactly half the time period between collapse and revival of the oscillations of atomic population inversion [13,14]; (c) generation of a Fock state by sending a sequence of excited atoms into the cavity and counting the number of atoms that have emerged in the excited state [6]. The limitation of this method is that it does not predict the eventual Fock state, but only the probability of its occurrence.

A recent approach, capable of yielding both Schrödinger cats and Fock states, is based on the detection of the dispersive field-induced phase shift acquired by the initially polarized state of nonresonant atoms in the cavity [15]. The random variation of these phase shifts with the atomic transit time (velocity) in a sequence of such measurements results in repeated splitting of the phase-space field distribution and interference between the split parts. The first step in the sequence yields a phase-difference Schrödinger cat, while subsequent steps gradually lead to phase diffusion and decimation (through interference) of the photon-number distribution, converging to a Fock state. Like the method of excited-atom counting described above [6], the random-phase-shift method cannot determine in advance the eventual Fock state.

In this paper we propose a scheme that allows the generation of a variety of nonclassical field states with *controllable* (predetermined) photon-number and phase distributions. It is based on the generalization of a recently proposed generation of Schrödinger cats with controll-

*Permanent address: Instituto Nacional de Astrofisica Optica y Electronica, Apartado Postal 51 y 216, Puebla, Puebla, Mexico.

able phase difference, by a *conditional* measurement of the atomic excitation (i.e., selection of excited-state outcomes), following its two-photon resonant interaction with the cavity field [16]. This generation is a result of the *correlation* between the selected atomic state and the cosinusoidally evolving Fock-state components of the field. The linear n dependence of the n-photon nutation frequency between the lower and the upper atomic states is responsible for the periodic, regular field evolution in the two-photon resonant model. Here we consider sequences of such measurements. Each measurement splits the phase-space field distribution created by the previous measurement into two identical parts whose mean phase difference is controlled by the atomic transit time. The field distribution, resulting from a sequence of N such measurements, is peaked about $2N$ positions in the phase plane, which evolve periodically as a function of the atomic transit times, and are therefore simply controlled. When these peaks are chosen not to overlap, the field state constitutes a $2N$-component generalized Schrödinger cat. Alternatively, by choosing them to overlap, we can make parts of the field distribution strongly interfere, giving rise to decimation of the photon-number distribution. One of the main achievements of this method is the efficient generation (by rather short atomic sequences) of *preselected* Fock states. It should be noted that nonclassical field generation by measurements of an atomic state has been considered by Agarwal *et al.* in a very recent work [17] concerning three-level atoms interacting with two fields, and resulting in a phase-squeezed state.

Another problem addressed by the present treatment is the detection of the nonclassical states described above. The detection scheme of Schrödinger cats in a cavity that has been previously proposed [15] is rather involved. Here we extend to many-atom sequences the suggestion of Refs. [16] and [18] for a one-atom Schrödinger cat detection. It is shown that the lumpiness of the generated multipeak phase distribution can be detected by monitoring the time dependence of the revivals in the excitation of an additional $N+1$ "probe" atom, following the sequence of N atoms that have generated the field state.

In Sec. II we review the results for "cats" created by one and two atoms, and then calculate their photon-number and phase distributions. In Sec. III we consider the generation of various nonclassical states by two types of conditional measurement sequences, namely, fixed interaction-time sequences, and sequences of decreasing interaction times. We then study the detection of the phase distribution by a "probe" atom. Finally, we consider the unavoidable effects of atomic velocity spread, thermal noise, and detection efficiency. Section IV summarizes the conclusions.

II. GENERATION OF SUPERPOSITION STATES BY INTERACTION WITH ONE AND TWO ATOMS

A. The model

The present model pertains to the interaction of an atomic beam with a single mode of an electromagnetic field in a cavity. We assume that there is only one atom at a time inside the cavity, and that the Q factor of the cavity is sufficiently high so as to neglect dissipative effects. Since our aim is to generate nonclassical field states (such as Schrödinger cats) that have $\bar{n}$ photons on the average, the effective relaxation time is the cavity lifetime reduced by a factor of $\bar{n}$ [11,19,20]. Hence, dissipation will be negligible for a sequence of atomic interaction times whose total duration is considerably shorter than this effective relaxation time. These requirements have been met in experimental situations realized in Ref. [7]. We consider two-photon resonant transitions in a cascade between atomic levels $|e\rangle \rightarrow |i\rangle \rightarrow |g\rangle$ (Fig. 1) such that the photon frequency ω satisfies $\omega_{eg}=2\omega$, whereas the intermediate transition frequencies ω_{ei} and ω_{ig} are strongly detuned from ω by $\Delta/2=\omega-\omega_{ei}=\omega_{ig}-\omega$. An important feature of these transitions is that the respective Rabi frequencies (per photon) Ω_{ei} and Ω_{ig} give rise to the Stark shifts $(n+1)\Omega_{ei}^2/\Delta$ (for the first transition) and $(n+2)\Omega_{ig}^2/\Delta$ (for the subsequent one). These Stark shifts can effectively counter the detunings $\pm\Delta/2$. Nevertheless, the intermediate state $|i\rangle$ can remain unpopulated during the interaction times t_j, and therefore be eliminated, provided that [21]

$$\frac{\Omega_n^2 t_j}{|\Delta|} \ll \pi, \quad j=1,2,3,\ldots,K \ . \tag{2.1}$$

Here Ω_n is the frequency [22] of the two-photon Rabi nutation corresponding to an n-photon Fock state between the ground ($|g\rangle$) and excited ($|e\rangle$) states:

$$\Omega_n = A + nB \ , \tag{2.2}$$

where

$$A=(\Omega_{ei}^2+2\Omega_{ig}^2)/\Delta, \quad B=(\Omega_{ei}^2+\Omega_{ig}^2)/\Delta \ . \tag{2.3}$$

The elimination of the intermediate state $|i\rangle$ makes it possible to consider our atom as an effective two-level system and use the solutions of the Jaynes-Cummings model on substituting Ω_n [given by Eq. (2.2)] instead of the ordinary Fock-state Rabi frequency, which scales as $(n+1)^{1/2}$. Starting with an excited atom and an arbitrary state of the field, the initial wave function of the system can be written as

$$|\Psi(0)\rangle = |e\rangle \sum_{n=0}^{\infty} c_0(n)|n\rangle \ . \tag{2.4}$$

We then perform a conditional measurement of the atomic excitation on the final entangled state of the system after the interaction. The particular conditional measurement chosen here consists of selecting a sequence

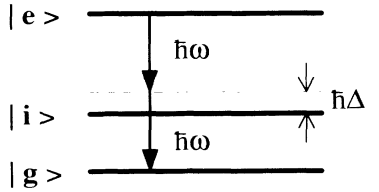

FIG. 1. Diagram of a two-photon transition via a cascade ("ladder") of two off-resonant dipole transitions.

of atoms, all of which emerge in their upper state. Each measurement in such a sequence is realizable with a high efficiency by the field ionization technique [7]. As shown in Ref. [16], the conditional measurement of the first atom projects the entangled state of the system onto a macroscopic quantum superposition state of the field (optical Schrödinger cat).

B. Single-atom "cat" state

The first atom evolves with the field for a time t_1 to a state $\Psi(t_1)$, and we observe the excited state with probability [16]

$$P_1=|\langle e|\Psi(t_1)\rangle|^2=\sum_{n=0}^{\infty}|c_0(n)|^2\cos^2\left[\frac{\Omega_{n+2}t_1}{2}\right]. \quad (2.5)$$

If we observe the state $|e\rangle$, then the corresponding field state is determined by the normalized projection $\langle e|\Psi(t_1)\rangle$,

$$|\psi_f(t_1)\rangle=\sum_{n=0}^{\infty}c_1(n)|n\rangle , \quad (2.6a)$$

where

$$c_1(n)=\frac{1}{\sqrt{P_1}}c_0(n)\cos\left[\frac{\Omega_{n+2}t_1}{2}\right] \quad (2.6b)$$

are new coefficients for the field distribution. This photon-number distribution $|c_1(n)|^2$ is normalized to unity, because the measurement is conditional on an excited atom being observed. For the case of an initial coherent state $|\alpha\rangle$

$$c_0(n)=\exp\left[-\frac{\alpha^2}{2}\right]\frac{\alpha^n}{\sqrt{n!}} , \quad (2.7)$$

when we choose α to be real. The expression (2.6a) can then be rewritten as [using (2.2)]

$$|\psi_f(\alpha,t_1)\rangle=\frac{1}{2\sqrt{P_1}}(e^{i(A+2B)t_1/2}|\alpha e^{iBt_1/2}\rangle + e^{-i(A+2B)t_1/2}|\alpha e^{-iBt_1/2}\rangle) . \quad (2.8)$$

The ket vector $|\psi_f(\alpha,t_1)\rangle$ is a quantum superposition of two coherent states with a relative phase Bt_1, and constitutes an optical Schrödinger cat [3]. Thus the evolution of the system from an initial coherent state followed by a measurement of the atomic excitation results in a superposition of coherent states with a phase controllable by t_1. This remarkable feature of the two-photon Jaynes-Cummings model provides a rather simple scheme for the preparation of macroscopic quantum superpositions by measurements on a single atom.

Our particular scheme of conditional measurements is used here only for convenience. Indeed, if the outgoing atom were found to be in its *ground* state, then the state of the field would have the form

$$|\psi_f(t_1)\rangle=\frac{1}{\sqrt{\tilde{P}_1}}\sum_{n=0}^{\infty}c_0(n)\sin\left[\frac{\Omega_{n+2}t_1}{2}\right]|n+2\rangle , \quad (2.9)$$

where $\tilde{P}_1$ is the appropriate normalization for this case. The field state (2.9) corresponds to a superposition analogous to (2.8). Hence, we only need to measure the atomic excitation to obtain a Schrödinger cat.

In order to prepare a macroscopic superposition, we can start at $t=0$ even from a *mixed state* of the field (see Ref. [16]), as long as it is characterized by a narrow quasiclassical distribution in phase and amplitude. This means that the initial density operator of the field, when written in the basis of coherent states $|\alpha'\rangle$,

$$\rho_f(0)=\int d^2\alpha' P(\alpha')|\alpha'\rangle\langle\alpha'| , \quad (2.10)$$

has a distribution $P(\alpha')$ that is localized around the coherent state $|\alpha\rangle$ with small normalized variances in phase and amplitude. A laser (or maser) well above threshold (yet well below the saturation limit) is a suitable example. It is easily checked that the Q function

$$Q_1(\beta,\beta^*)=\frac{1}{\pi}\langle\beta|\rho_f(t_1)|\beta\rangle = \frac{1}{\pi}\langle\psi_f(\beta,t_1)|\rho_f(0)|\psi_f(\beta,t_1)\rangle , \quad (2.11)$$

evolving from $\rho_f(0)$ of (2.10), consists of two diagonal parts peaked around the states $|\alpha\exp(iBt_1/2)\rangle$ and $|\alpha\exp(-iBt_1/2)\rangle$. Each part is described by the initial Q function rotated either clockwise or counterclockwise by the phase $Bt_1/2$.

The photon-number and phase distribution of a given (instantaneous) superposition of the type (2.8) were investigated by Schleich, Pernigo, and Kien and Bužek, Vidiella-Barranco, and Knight [3]. Here we study the dynamical evolution of these properties for our two-photon resonant conditional "cat" state.

One manifestation of the nonclassical properties of our cat state can be seen in its photon statistics: The mean values $\langle\hat{n}\rangle$ and $\langle\hat{n}^2\rangle$ are given by

$$\langle\hat{n}(t_1)\rangle\equiv\langle\psi_f(t_1)|a^\dagger a|\psi_f(t_1)\rangle = \frac{\alpha^2}{2P_1}(1+\exp\{\alpha^2[\cos(Bt_1)-1]\}\cos[\alpha^2\sin(Bt_1)+(A+3B)t_1]) , \quad (2.12)$$

$$\langle\hat{n}(t_1)^2\rangle=\langle\hat{n}(t_1)\rangle+\langle\psi_f(t_1)|(a^\dagger)^2a^2|\psi_f(t_1)\rangle = \langle\hat{n}(t_1)\rangle-\frac{\alpha^4}{2P_1}(1+\exp\{\alpha^2[\cos(Bt_1)-1]\}\cos[\alpha^2\sin(Bt_1)+(A+4B)t_1]) . \quad (2.13)$$

It was shown for the single-photon JCM [9] that the normalized uncertainty of the photon number

$$\sigma=\left[\frac{\langle\hat{n}^2\rangle-\langle\hat{n}\rangle^2}{\langle\hat{n}\rangle}\right]^{1/2}\equiv\frac{\Delta\hat{n}}{\sqrt{\langle\hat{n}\rangle}} \tag{2.14}$$

rapidly oscillates as a function of t_1. In fact, as we now know, this occurs whenever the coherent states of the superposition overlap in phase space. Similar behavior is exhibited by Eq. (2.13) for the two-photon JCM in the vicinity of $Bt_1=2\pi$ [Fig. 2(a)]. Values of σ below unity in Fig. 2(a) correspond to the state having sub-Poissonian photon statistics. The region of squeezing coincides with that of sub-Poissonian statistics. As implied by Eq. (2.13), these nonclassical properties result from the overlap and interference of the superposition parts.

We note that in general $\langle\hat{n}(t_1)\rangle$ is not equal to α^2. Thus after a conditional measurement the mean energy of the field may be changed, even though the measured atom enters and leaves the cavity in the same (excited) state. This is not surprising if we bear in mind that there is no conservation of the *mean* energy. The initial state is not a number state with definite energy but a photon-number distribution. The observation of an excited outgoing atom selects certain components of the distribution by virtue of their correlation (at time t_1) to the atomic state $|e\rangle$. If $\bar{n}_e$ and $\bar{n}_g$ are the mean photon numbers for the excited and ground states, respectively, then we have $\alpha^2=P_1\bar{n}_e+(1-P_1)\bar{n}_g$, with P_1 given by Eq. (2.5).

The phase distribution of the field is described in the Pegg-Barnett formalism [23] by the function

$$F_1(\theta)=\frac{1}{2\pi}\left|\sum_{n=0}^{\infty}c_1(n)e^{-in\theta}\right|^2 . \tag{2.15}$$

The phase distribution of $|\psi_f(\alpha,t_1)\rangle$ and the corresponding Q function [Eq. (2.11)] are given in Figs. 2(b) and 2(c). Here and hereafter we set $A=B$ in all our plots. The two peaks of our quantum superposition are observed very clearly. The relative phase between the superposition parts Bt_1 is linear in the interaction time and is independent of the field intensity, due to the two-photon character of the transitions.

Throughout this paper we illustrate the field state by the Q (or Husimi) probability distribution function. Of course, we could have used other quasiprobability functions. The Wigner function, for example, would clearly show the presence of a superposition by exhibiting interference fringes between the peaks of the distribution.

C. Second-atom cat-state production: satellite revivals

We have seen that the first atom splits a coherent-state Q function into two identical parts with shifted phases. "Revivals" in the oscillation pattern of the atomic population occur every time the ratio $\varphi/2\pi$ attains integer values, corresponding to complete overlap of the Q-function parts. The second atom is expected to split each of the new coherent-state parts into two identical parts again, yielding a four-peaked Q function.

The second atom enters the cavity after the first one leaves, and interacts with the field for time t_2. The

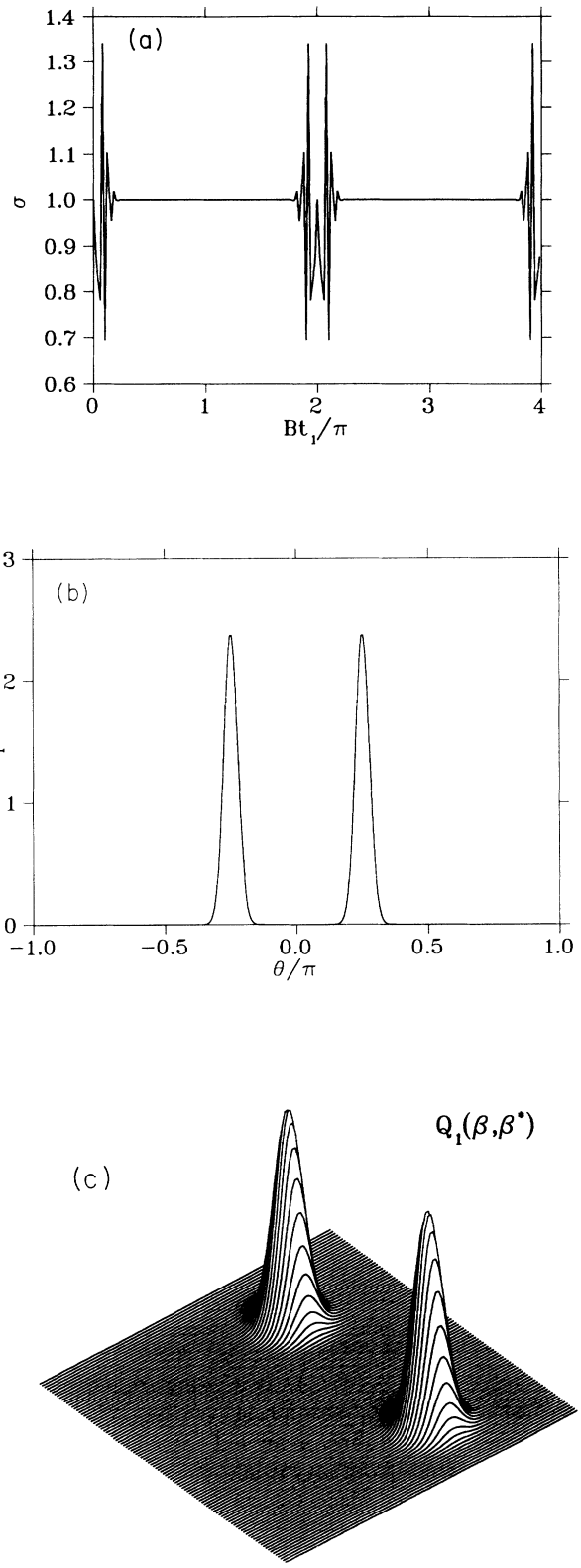

FIG. 2. (a) Normalized photon-number uncertainty σ as a function of the dimensionless atomic transit time. Collapses and revivals of Rabi oscillations occur in the vicinity of $Bt_1=2N\pi$. (b) Phase distribution and (c) corresponding Q function of a quantum superposition (optical Schrödinger cat) generated from an initially coherent state by a conditional measurement on the emerging atom for $Bt_1=\pi/2$.

overall probability of having two consecutive excited atoms is, using (2.6b),

$$P_2=P_1\sum_{n=0}^{\infty}|c_1(n)|^2\cos^2\left[\frac{\Omega_{n+2}t_2}{2}\right]$$
$$=\sum_{n=0}^{\infty}|c_0(n)|^2\cos^2\left[\frac{\Omega_{n+2}t_1}{2}\right]\cos^2\left[\frac{\Omega_{n+2}t_2}{2}\right]. \quad (2.16)$$

If again we assume the field at $t=0$ to be in a coherent state, the probability P_2 displays novel dynamics as a function of t_2, namely, pairs of "satellite" revivals appear in addition to the regular ones [16] (compare with Ref. [18]) [Fig. 3(a)]. This can be seen if we substitute the $c_0(n)$ from Eq. (2.7) into Eq. (2.16), and rewrite the cosine factors on the right-hand side of Eq. (2.16) in the form

$$\cos^2\left[\frac{\Omega_{n+2}t_1}{2}\right]\cos^2\left[\frac{\Omega_{n+2}t_2}{2}\right]$$
$$=\frac{1}{4}\left[1+\cos(\Omega_{n+2}t_1)+\cos(\Omega_{n+2}t_2)+\frac{1}{2}\cos[\Omega_{n+2}(t_2-t_1)]+\frac{1}{2}\cos[\Omega_{n+2}(t_2+t_1)]\right]. \quad (2.17)$$

Each of the four cosine terms in Eq. (2.17) produces a distinct set of revivals in (2.16). This means that revivals in P_2 appear at the times

$$Bt_2, B(t_2\pm t_1)=2\pi N\ , \quad (2.18)$$

where N is an integer. The amplitude of each satellite revival is half of the regular one. These satellite revivals are shifted by $\pm Bt_1$ from the regular revivals. The same features are revealed by the closed form of P_2,

$$P_2(t_2)=\frac{1}{2}+\sum_{j=0,\pm1}N_\alpha^{-1}(t_1)e^{-\alpha^2}\exp\{\alpha^2\cos[B(t_2+jt_1)]\}$$
$$\times\cos\{(A+2B)(t_2+jt_1)+\alpha^2\sin[B(t_2+jt_1)]\}\ , \quad (2.19)$$

where

$$N_\alpha(t)=2+2\cos[\alpha^2\sin(Bt)]\exp[-2\alpha^2\sin^2(Bt/2)]\ . \quad (2.20)$$

Thus we have a straightforward method for the detection of the cat phase in the same setup that serves for its generation, by monitoring the excitation probability of the second atom as a function of its interaction time (or velocity).

Let us examine the field state after the conditional measurement on the second atom. This state, which must be normalized by the probability P_2, has the form

$$|\psi_f(t_1,t_2)\rangle=\sum_{n=0}^{\infty}c_2(n)|n\rangle$$
$$=\sum_{n=0}^{\infty}\frac{c_0(n)}{\sqrt{P_2}}\cos\left[\frac{\Omega_{n+2}t_1}{2}\right]$$
$$\times\cos\left[\frac{\Omega_{n+2}t_2}{2}\right]|n\rangle\ . \quad (2.21)$$

If the initial field is coherent, then, as we have mentioned already, the resulting distribution in the phase plane has in general four peaks (if t_2 does not coincide with the periods of t_1 revivals, otherwise some of the peaks overlap). The phase distribution $F_2(\theta)=(1/2\pi)|\sum_{n=0}^{\infty}c_2(n)e^{-in\theta}|^2$ and the Q function $Q_2(\beta,\beta^*)$ are shown in Figs. 3(b) and 3(c). Let us consider a cat, produced by a second observation of an excited atom in the special case $Bt_1=\pi$ (maximal separation of superposition components). In Fig. 4 the evolution of this cat is plotted at $Bt_2=0$ (original state), $Bt_2=\pi/2$ (four peaks), and $Bt_2=\pi$ (the same state, rotated by $\pi/2$). We can see from Eq. (2.18) that for $Bt_1=\pi$ the satellite revivals overlap completely, resulting in a double rate of revivals with equal amplitudes.

III. GENERATION AND DETECTION OF NONCLASSICAL STATES BY MANY-ATOM SEQUENCES

A. Motivation

It is easy to generalize the foregoing treatment to conditional excitation measurements on K atoms. The resulting state of the field is

$$|\psi_f(t_1,\ldots,t_K)\rangle=\sum_{n=0}^{\infty}c_K(n)|n\rangle\ , \quad (3.1)$$

where

$$c_K(n)=\frac{c_0(n)}{\sqrt{P_K}}\prod_{j=0}^{K}\cos\left[\frac{\Omega_{n+2}t_j}{2}\right] \quad (3.2)$$

and the probability to have K excited atoms is

$$P_K=\sum_{n=0}^{\infty}|c_0(n)|^2\prod_{j=1}^{K}\cos^2\left[\frac{\Omega_{n+2}t_j}{2}\right]. \quad (3.3)$$

The coefficients of the distribution satisfy the normaliza-

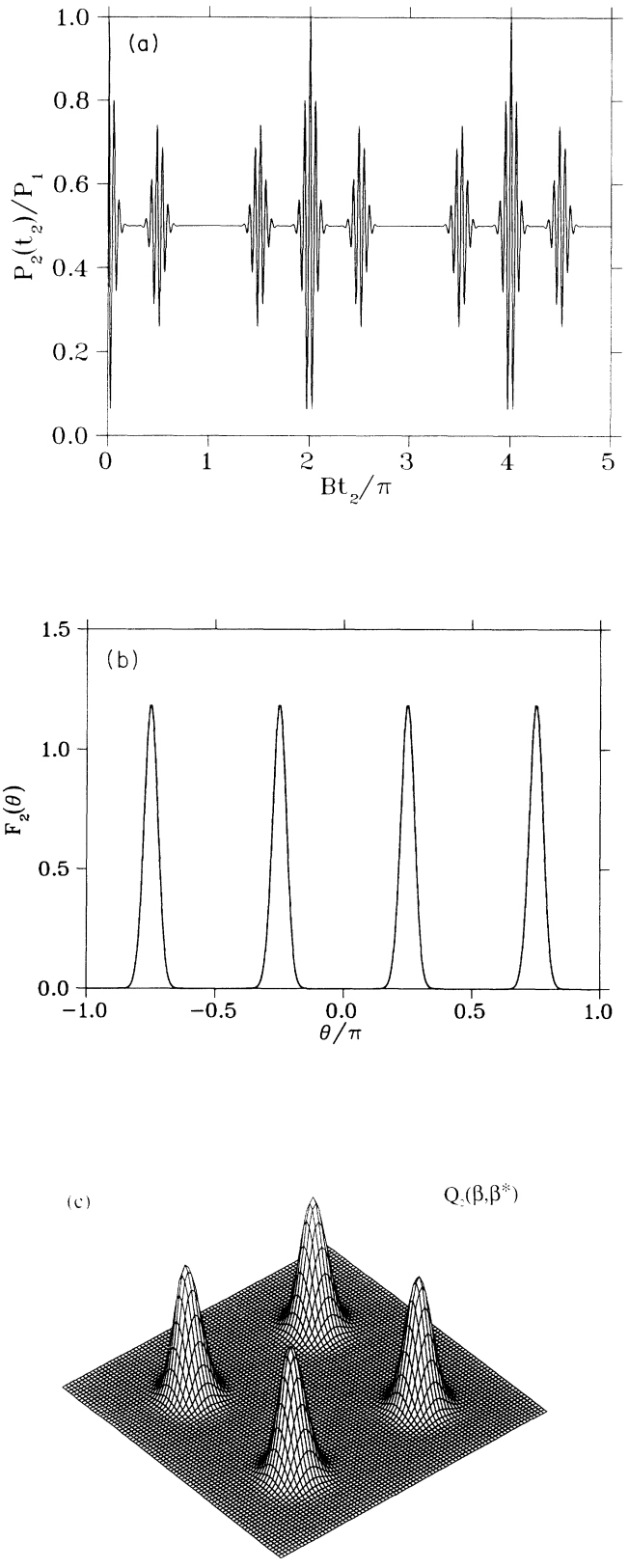

FIG. 3. (a) Excitation probability of a second atom as a function of its interaction time Bt_2 after a conditional measurement on the first atom. "Satellite" revivals (in addition to the regular ones) are displayed ($Bt_1=\pi/2$). (b) Phase distribution and (c) the Q function of the field after a conditional measurement on the second atom. ($Bt_2=\pi$).

tion condition:

$$\sum_{n=0}^{\infty} |c_K(n)|^2=1 \ . \tag{3.4}$$

We have seen in the case of two atoms that the initial coherent state evolves into a distribution whose four peaks (circular lumps) have different mean phases and a common mean amplitude ("radius"). This distribution

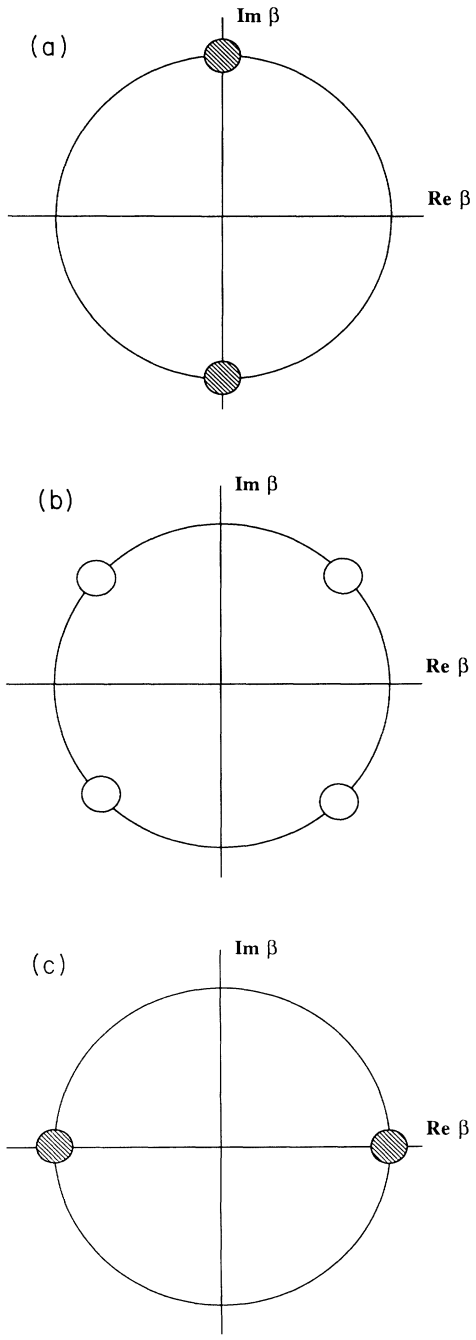

FIG. 4. Evolution of an optical Schrödinger cat interacting with the second excited atom in the case of superposition phase $Bt_1=\pi$: (a) the same cat ($Bt_2=0$), (b) a four-peaked field distribution after interaction time $Bt_2=\pi/2$, (c) the same cat rotated by $\pi/2$ after $Bt_2=\pi$.

exhibits sub-Poissonian photon statistics when two or more peaks overlap. One may ask whether a longer sequence of excited-atom observations can generate qualitatively different distributions, whose structure yields *controlled* values of photon number or phases. The effectiveness of such generation is measured by the length (duration) as well as by the joint probability of the required sequence P_K.

First we look at what happens if the interaction times are constant. A real atomic beam is never perfectly monochromatic, so that the scheme of fixed interaction times can be considered as a first approximation to the problem. We then discuss the case of decreasing interaction times, corresponding to a sequence in which every atom passes the cavity faster than the previous one. We choose a particular case where successive interaction times are halved, so that the initial coherent state is rapidly redistributed over a ring in the phase plane. By this means we hope to simulate the phase-space distribution of a Fock state. Finally we consider the smearing of interaction times by a Gaussian distribution of velocities.

B. Fixed interaction times

In Fig. 5 we see the photon numbers and phase distributions, when interaction times are $Bt_j = 0.3\pi$ for all $t_j = t_1, t_2, \ldots, t_K$ up to $K = 24$ atoms. There is a suppression of part of the number distribution corresponding to the vanishing of the product of cosines in Eq. (3.3) at particular values of n. After $K = 100$ atoms the number distribution is close to a number state. However, the phase distribution still remains lumpy, because each coherent state splits by the angle 0.3π, which results in repetition of the pattern after approximately $K = 40$ atoms (or "splittings").

If we wish to obtain a uniform phase distribution as in a genuine Fock state, it is best to choose a smaller splitting angle $Bt_j \ll 1$, so that the parts of the distribution

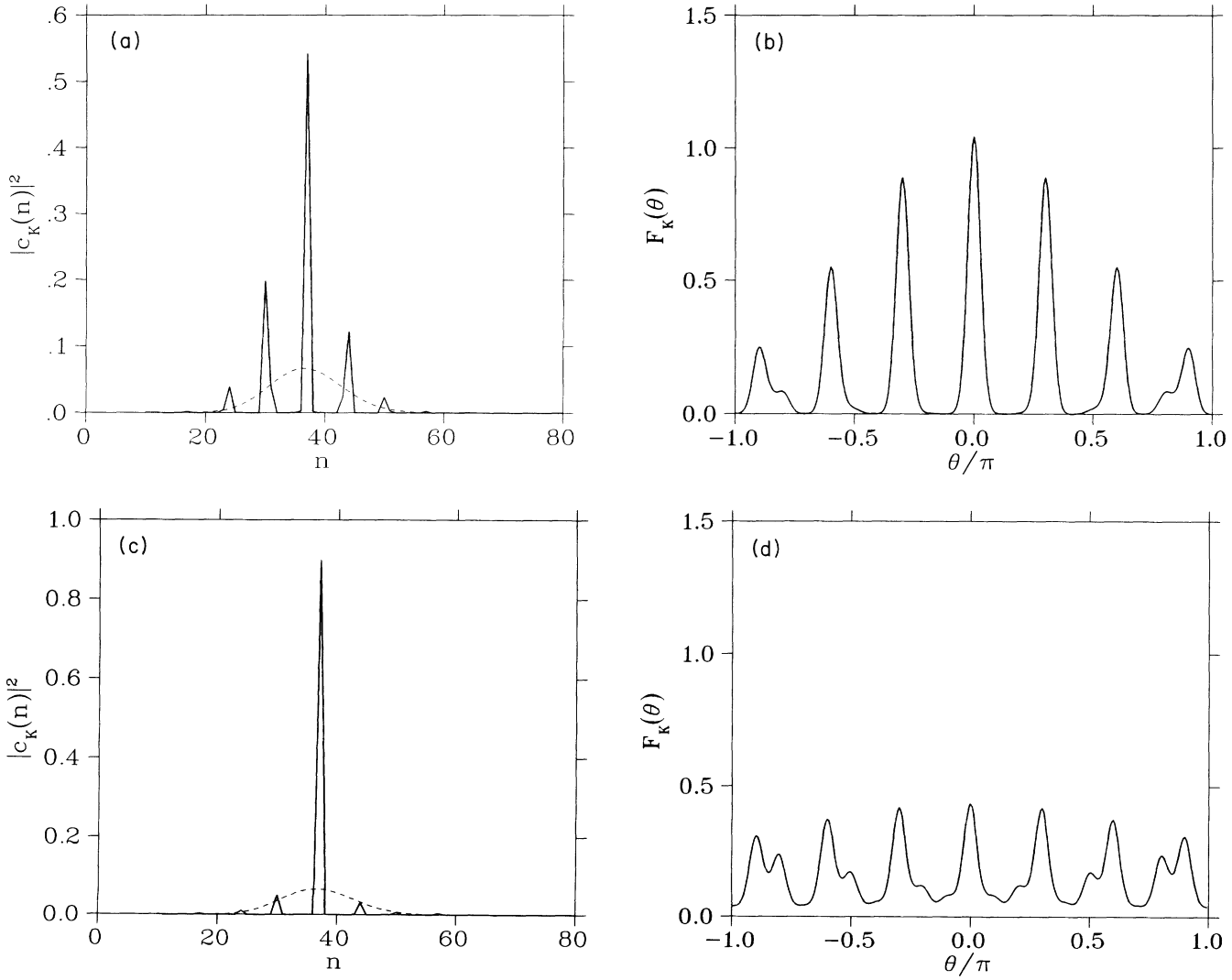

FIG. 5. The photon-number and phase distributions of the field following sequences of excited-atom conditional measurements for large fixed interaction times $Bt_j = 0.3\pi$. (a) Solid line—the photon-number distribution after $K = 24$ excited atoms. Dashed line—the initial Poissonian distribution with $\alpha = 6$. (b) The phase distribution after $K = 24$ excited atoms. (c) The photon-number distribution after $K = 100$ atoms. (d) The phase distribution after $K = 100$ atoms.

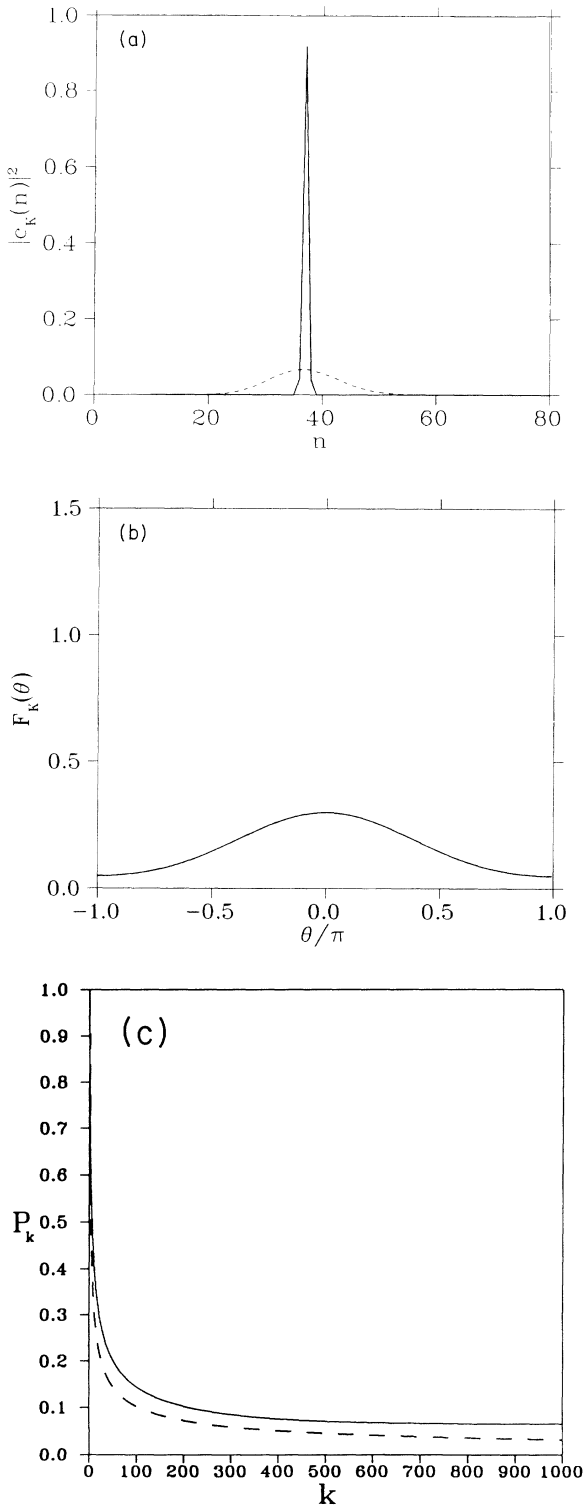

FIG. 6. Results for sequences of excited-atom conditional measurements with short fixed interaction times $Bt_j=0.05\pi$. (a) Photon-number distribution showing Fock-state generation for $K=500$ excited atoms from a coherent initial state with $\alpha=6$ (shown dashed). (b) The phase distribution of the generated field for the same parameters. (c) The probability P_K of finding a sequence of excited atoms as a function of their number K, for the same parameters. Dashed curve—our approximation [Eq. (A5)]; solid curve—numerical evaluation without approximation.

overlap in the phase plane after each splitting. As an example, we have set $Bt_j=0.05\pi$. After 100 atoms the number distribution is confined to a narrow range and the phase distribution contains a broad peak. As the number of atoms increases, the phase distribution diffuses and the number distribution sharpens up. In Fig. 6 we have an almost pure Fock state and a nearly flat phase distribution, after 500 atoms.

It is quite relevant to ask how likely we are to observe such long sequences of excited atoms. The sequence probability P_K [Eq. (3.3)] is an infinite sum of products. Nevertheless, we can carry out the infinite sum in the case of fixed times for an initial coherent state $|\alpha\rangle$. As shown in the Appendix, we may also derive the following estimate for large K:

$$P_K=\frac{(2K!)}{2^{2K}(K!)^2}\left[1+2e^{\alpha^2[\cos(B\tau)-1]}\times\cos[\alpha^2\sin(B\tau)+(A+2B)\tau]\times\frac{K}{K+1}\right]. \tag{3.5}$$

We have plotted both the exact and estimated expressions for P_K in the case $Bt_j=0.05\pi$ [Fig. 6(c)]. We can see that as the number of atoms K increases there is a rapid initial fall in probability, which flattens out eventually. After 100 atoms we obtain a value of $P_K\approx 0.1$, which is very slowly decreasing with K. Hence, as the number of atoms increases we are more likely to observe an excited atom at each step. This comes about because the K-fold product of the cosine factors in Eq. (3.3) diminishes the contributions from each n value at different rates. As the number of atoms K becomes large, the rapidly diminishing terms die out, leaving only a single long-lived n-state contribution to P_K. This n state corresponds to the value of $\cos^2(\Omega_n t/2)$ nearest to 1. Thus we have a rather reliable method for producing a number state, which will succeed for about one in ten experimental runs.

C. Decreasing interaction times

In order to reduce the length of the sequence that yields a number state of the field, and thereby avoid the need for a very-high-Q value, we suggest the scheme of decreasing interaction times. Let us define the time sequence as

$$Bt_j=\frac{\pi}{2^{j-1}},\quad j=1,\ldots,K, \tag{3.6}$$

so that the passage time is reduced by one-half after each pass.

The first atom creates a cat with two components separated in phase by π. The second atom creates four components separated by $\pi/2$. The third atom pass will result in eight evenly spaced components and so on. When the number of atoms is only six, the phase distribution becomes smooth, indicating that we might have a number state. In order to check this surmise, we examine the photon-number distribution obtained from Eq. (3.3)

(Fig. 7). As the number of atoms increases, the photon-number distribution is decimated and a Fock state is achieved at $n=29$ after five atoms for an initial $\langle n \rangle = 36$. However, if we add a sixth atom, the number state jumps from $n=29$ to 61.

The key to this process lies in the behavior of the cosine factors in Eq. (3.3). For the nth component of the distribution we have the product

$$|c_K(n)|^2 = \frac{|c_0(n)|^2}{P_K} \cos^2\left[\frac{\Omega_{n+2}t_1}{2}\right] \cos^2\left[\frac{\Omega_{n+2}t_2}{2}\right] \times \cdots \cos^2\left[\frac{\Omega_{n+2}t_K}{2}\right] \tag{3.7}$$

after K atoms. If we take for the sake of simplicity $A=B$, then

$$\cos^2\left[\frac{\Omega_{n+2}t_j}{2}\right] = \cos^2\frac{(n+3)\pi}{2^j} . \tag{3.8}$$

This factor is zero if

$$(n+3)\pi/2^j = \pi(l+1/2) , \tag{3.9}$$

where l is any integer. Thus after the jth atom we lose all the n components of the distribution which satisfy

$$n = 2^{j-1}m - 3 , \tag{3.10}$$

where the factor m is any odd number such that $n \geq 0$. We lose $n=0,2,4,\ldots$ for $j=1$, $n=3,7,11,\ldots$ for $j=2$, and $n=1,9,17,\ldots$ for $j=3$. Hence, the remaining components are

$$\begin{aligned} &n=13,29,45,\ldots \quad \text{for } K=4 , \\ &n=29,61,93,\ldots \quad \text{for } K=5 , \\ &n=61,125,189,\ldots \quad \text{for } K=6 . \end{aligned} \tag{3.11}$$

This explains the apparent "jump" in Fig. 7(d): $n=29$ dominates after five atoms, because of the ratios in the original distribution with $\langle n \rangle = 36$. Thus $n=61$ is not seen until $n=29$ is removed with the sixth atom. This "jump" to $n=61$ occurs with extremely low probability (the contribution of the component $|c_0(61)|^2$ to the initial field distribution is very small), i.e., it is very unlikely to find the sixth atom in its excited state.

This method is quite efficient at attaining a number state. It very rapidly reduces the initial Poissonian distribution to the final number state by decimating the

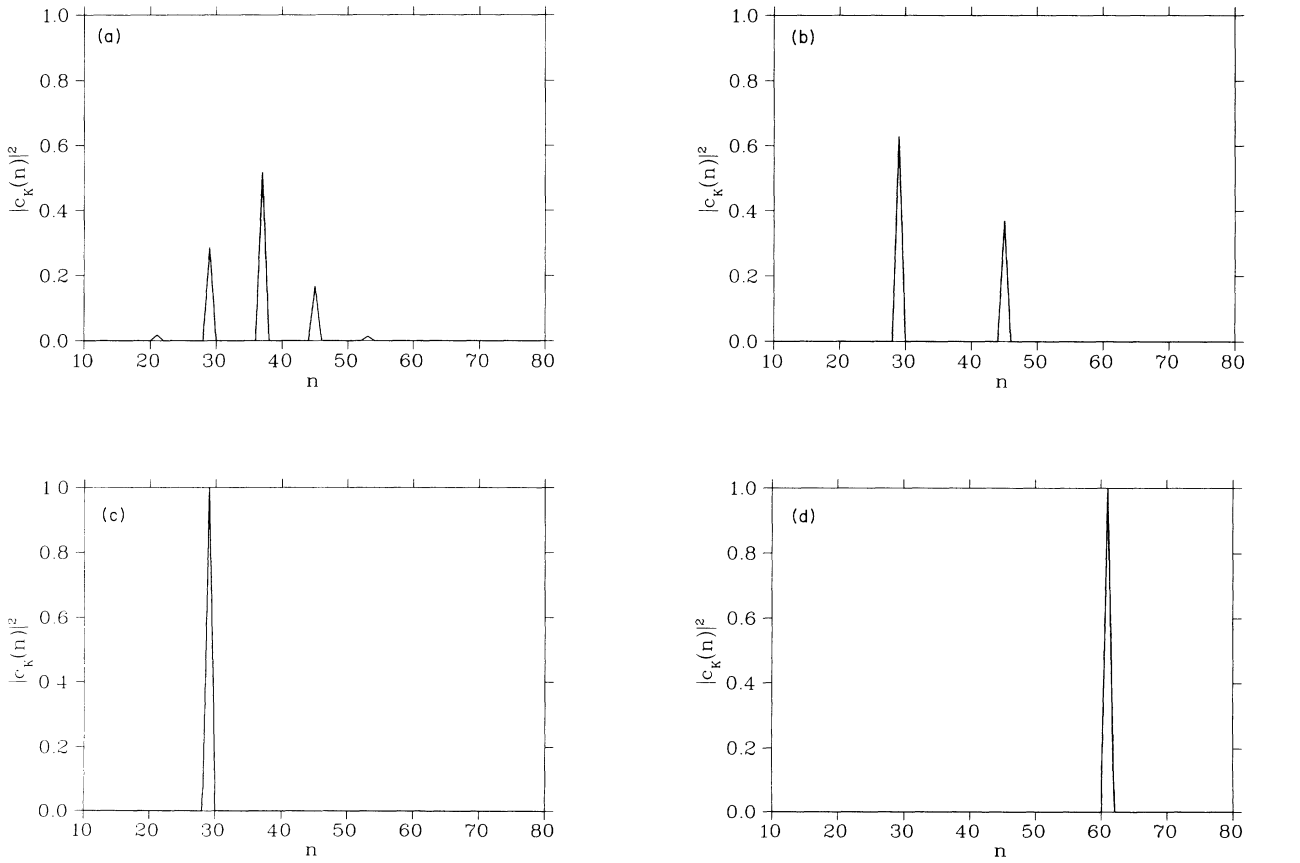

FIG. 7. A sequence of excited-atom conditional measurements with successively halved interaction times, starting with $Bt_1=\pi$ [Eq. (3.6)]. The field is initially coherent with $\alpha=6$. (a) The photon-number distribution after three excited atoms (eight-component Q function). (b) The same after four excited atoms—a coherent superposition (Schrödinger cat) of two different photon numbers $n=29$ and 45. (c) The same after five excited atoms—an approximate Fock state with $n=29$ is generated. (d) The distribution after six excited atoms, corresponding to a very unlikely jump of the number state from $n=29$ to 61.

photon-number distribution. A specially designed velocity selector is needed to supply such a sequence. However, it is not as difficult as the selector suggested by Krause *et al.* [6] for the ordinary (one-photon) JCM, which requires velocity increments by *irrational* factors (scaling as $n^{-1/2}$).

D. Superpositions of distinct number states

In Fig. 7(b) we see that after four atoms two main peaks have survived in the number distribution. The resulting state of the field is, in fact, a new example of a superposition state, analogous to an optical Schrödinger cat. In contrast to the usual phase-difference cats, this is a coherent superposition of two states with different photon numbers n_1 and n_2, which can be, in principle, macroscopic.

E. Detection of the multipeak phase distribution

The lumpiness of the phase distribution in Fig. 5 can be effectively detected using the same experimental setup by monitoring the excitation probability of a "probe" atom as a function of its interaction (transit) time. The multipeak phase distribution (multiple Schrödinger cats) in its interaction with such an atom produces partial revivals in the oscillation pattern of the atom population inversion. The pattern of inversion revivals contains all the information necessary to reconstruct the field phase distribution. The ordinary two-photon revivals (the field being initially in coherent state) occur with the period $T_R = 2\pi/B$. Interaction with a multiply peaked Schrödinger cat leads to as many revivals over this interval as the number of peaks in the field distribution [Fig. 8(a)]. The time interval between two neighboring revivals corresponds to the mean phase difference between two adjacent Q-function parts $B(t_{R1} - t_{R2})$.

As the field distribution approaches a photon-number state, the peaks in the phase distribution overlap, and so do the revivals of the atomic inversion, thereby becoming less pronounced [Fig. 8(b)]. In the case of a pure Fock state of the field, the atomic inversion displays Rabi oscillations at the frequency $\Omega_n = A + nB$ without any collapses and revivals, as it should.

F. Effect of a spread of interaction times (or velocities)

The following question arises: how stable is the procedure described above against thermal fluctuations in the atomic beam velocity? The Q-function splitting angles are sensitive to such fluctuations, so that random deviations of the interaction times may change the process dynamics in the following ways: (a) the phase "diffusion" of the field state may become more effective; (b) the realization of a sequence of excited atoms may become less probable. In order to investigate this problem we have performed a computer simulation of a thermal beam of atoms assuming a random Gaussian spread of interaction times. The present performance of velocity selectors provides monochromatic atomic beams with an accuracy of 1%. We therefore choose the width of our distribution to be 1% of the mean interaction time (the transit time through the cavity). For the fixed-times scheme the thermal fluctuation exponentially reduces the probability P_K, but the parameters of the resulting field are immune to these fluctuations. The best results are obtained for a small splitting angle (short interaction times). For example, the field distribution in Fig. 6 does not change for fluctuations of 1–2%, but the probability drops from 7×10^{-2} down to 10^{-2}.

In Fig. 9(a) we show the probability of realizing 1000 measurements of $|e\rangle$ as a function of the mean interaction time $B\bar{t}$. The velocity fluctuations are 1% of the mean. We can see a window in the range of values of $B\bar{t}$ in which there is a 1–2% probability of obtaining the required sequence of excited atoms. Figure 9(b), which shows the corresponding values of $\bar{n}$, demonstrates that there is quite a wide range of photon numbers n obtain-

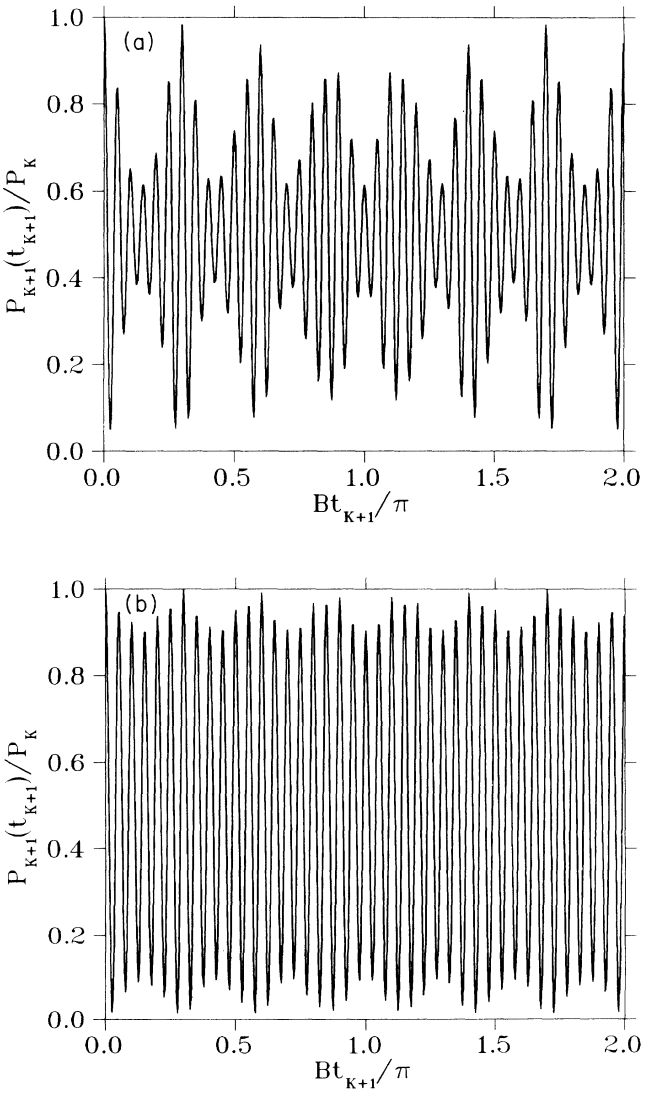

FIG. 8. Detection of the multipeak phase distribution by monitoring the excitation-probability revivals of a "probe" atom. (a) Revivals of the excitation oscillation of a probe atom for a field with the same parameters as in Figs. 5(a) and 5(b). (b) Revivals of a probe atom in a field with the parameters of Figs. 5(c) and 5(d).

able within this window ($30<n<50$). As the parameter $B\bar{t}$ is changed we step from one integer value of $\bar{n}$ to another, indicating that we generate a Fock state at each step. This is confirmed by Fig. 9(b), which shows that the values of Δn are exceedingly low in the stepping region, i.e., the states are highly sub-Poissonian.

The value of n that dominates the field distribution in Fig. 9(b) within the window discussed above is given by

$$\frac{\Omega_{n+2}\bar{t}}{2}=\frac{B(n+3)\bar{t}}{2}=\pi\ , \tag{3.12}$$

for which the K-fold cosine product in (3.3) is unity. However, for very small $B\bar{t}$ it is possible for low-n Fock states to dominate, because $|c_0(0)|^2\cos^{2K}(\Omega_2\bar{t}/2)$ can be larger than $|c_0(n)|^2\cos^{2K}(\Omega_{n+2}\bar{t}/2)$ with $n\gg 1$. The value of $B\bar{t}$ below which Eq. (3.12) is only satisfied by n far outside the original distribution corresponds to an instability point, at the remarkable sharp edge of the $\bar{n}$ distribution in Fig. 9(b). Evidence of this sharp-edge instability is seen in Fig. 9(c) where Δn exhibits a super-Poissonian upsurge, while being almost zero (strongly sub-Poissonian) throughout the "window." Note that

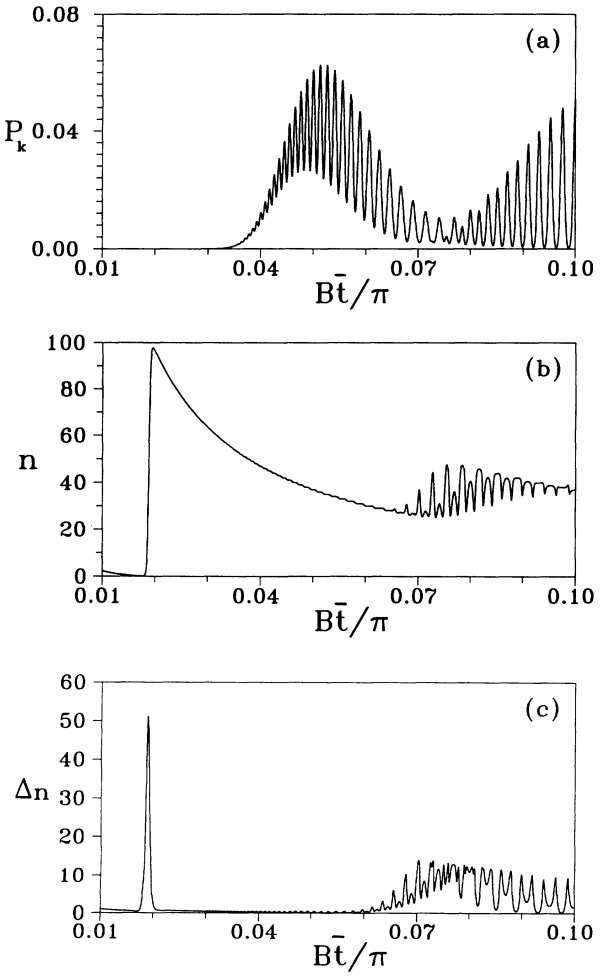

FIG. 9. (a) Sequence probability P_K, (b) mean photon number $\bar{n}$, and (c) the photon-number uncertainty Δn, for $K=500$, as a function of the mean (fixed) interaction time $B\bar{t}/\pi$, for 1% velocity (interaction time) fluctuations.

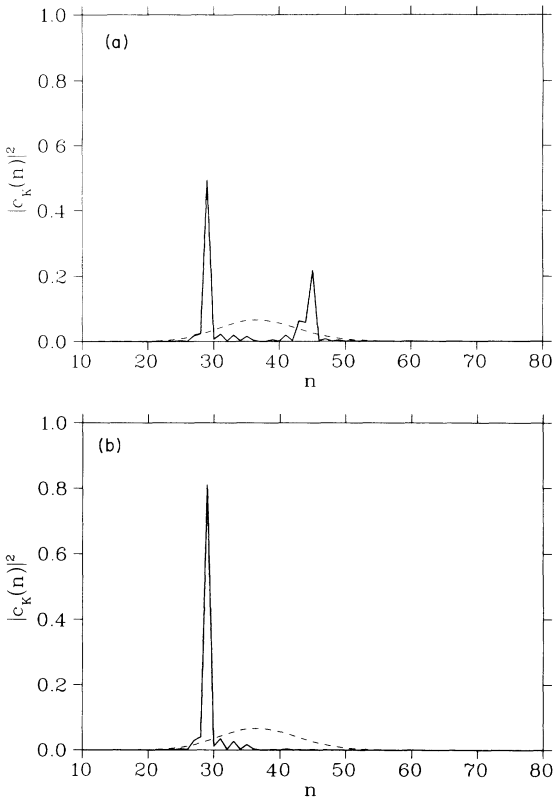

FIG. 10. Effects of thermal velocity fluctuations on the field in the successively halved interaction-times scheme. (a) The photon-number distribution after four-excited atoms, for fluctuations of 1%. All the parameters are as in Fig. 7. The sequence probability is $P_K=6\times10^{-2}$. The dashed line indicates the initial photon-number distribution. (b) The same, after $K=5$ excited atoms [compare with Fig. 7(c)]; the corresponding value of P_K is 3.5×10^{-2}.

these results are essentially independent of the size of velocity fluctuations, as long as they do not exceed roughly 5%.

The decreasing interaction-times scheme is also quite immune to fluctuations of this order. In Fig. 10(a) we can see the influence of a thermal distribution on the resulting field after a sequence of four atoms [compare with Fig. 7 (b)]. Figure 10 (b) demonstrates the possibility of Fock-state generation in the presence of thermal fluctuations. The field is still peaked at the same number state as without fluctuations ($n=29$).

G. Detection efficiency

Unwarranted field states can be obtained in the present scheme only by failing to record the passage of one or more atoms through the cavity, primarily due to imperfect detection efficiency in the field ionization scheme [15,22,24]. Hence, high-efficiency detectors are needed to keep the probability of Fock-state generation near the level calculated above, without losing too many atomic sequences due to detection imperfection. However, an important merit of this scheme is that once a sequence is recorded as successful (i.e., all atoms come out in the excited state), then its reliability can be tested by detecting

several additional "probe" atoms. If indeed the field has successfully converged to a Fock state, then all these probe atoms should come out in the excited state, as discussed in Secs. III B and III C. Conversely, the sequence should be discarded if some of the probe atoms are found to be unexcited, in order to eliminate the corresponding unwarranted field states.

IV. CONCLUSIONS

The present treatment has demonstrated the conceptual and calculational simplicity and effectiveness of the proposed conditional measurements of atomic excitation, as a means of generating and detecting preselected Schrödinger cats and Fock states. This simplicity stems from the advantageous properties of the two-photon resonant interaction, which results in splitting of the field Q function into two *identical* parts by each measurement, and their subsequent counter-rotation at a *constant* rate (simple sinusoidal evolution). The measurement sequences that have been studied in this paper have revealed that the transformation from a coherent state to a number state does not proceed by the mean-phase dissipation, but rather by decimation of photon-number components in the repeatedly split phase distribution. The phase distribution exhibits a regular structure during the process, with *mutual coherence* among its multiple components.

The specific features of the proposed measurement sequence are as follows.

(a) Fixed interaction-times sequences of ~ 100 atoms can yield a Fock state near the peak of the initial Poissonian distribution. The rate of sequence realization is $\sim 10\%$.

(b) Decreasing interaction-times sequences in which the transit time is halved by each subsequent atom reduce the field very rapidly (after approximately five atoms) to the preselected Fock state. The controllable coherence between the Fock-state components allows the generation of distinct superpositions of Fock states by only four atoms (compared with the large number of atoms required to produce a trapping state, which is a superposition of the vacuum and a number state [12]).

(c) The multipeak phase distribution of a generalized Schrödinger cat created by K atoms may be detected by the $K+1$ atom. The separation between adjacent satellites in the "revivals" pattern of this atom may reveal the mean-phase difference between neighboring peaks in the distribution, and indicate the gradual approach towards a Fock state.

(d) Our results are remarkably immune to thermal velocity spread. Thermal fluctuations of 1–2 % still allow the selection of various quantum states of the field (Fock states or Schrödinger cats) with *predictable* parameters. The possibility of abrupt switching from a very low to a very high Fock state by fine tuning of the interaction time in the presence of of thermal fluctuations is particularly intriguing.

(e) The main advantage of choosing conditional measurements of atoms in the $|e\rangle$ state rather than the $|g\rangle$ state is that the results are not spoiled, but merely discarded, if atoms decay to a lower state prior to detection. The possibility to test the result of each sequence by detecting additional "probe" atoms in the $|e\rangle$ state (Sec. III G) makes this scheme very reliable.

(f) Finally, we comment on the experimental conditions for the implementation of our scheme. The main requirement for the generation of a Fock state $|n\rangle$ is that the cavity lifetime $t_{\rm cav}=Q/\omega$, where Q is the quality factor, be much longer than n times the sequence duration $t_{\rm seq}$, which can be estimated as $t_{\rm seq}\geq 2\pi/B$ for both fixed-times and halved-times sequences, as shown in Secs. III B and III C (essentially, $t_{\rm seq}$ is the time needed to redistribute the multiply split Q function over a ring in the phase plane). In micromasers [22,24] operating on the two-photon rubidium transition $|40S\rangle\rightarrow|39P\rangle\rightarrow||39S\rangle(\omega_{eg}/2\pi=68.415$ GHz) with $\Delta/2\pi=-39$ MHz in a cavity of volume $V\approx 70$ mm^3, we have $B=4000$ s^{-1}, and therefore $t_{\rm seq}\geq 10^{-3}$ s. The requirement $t_{\rm cav}\gg nt_{\rm seq}$ then amounts to $Q\gg n\times 10^9$, which is compatible for $n\leq 50$ with currently achievable quality factors of 10^{12} in superconducting microwave cavities [7]. The single-atom interaction times under the quoted conditions are $t_j\geq 10^{-5}$ s in the fixed-times scheme ($K\sim 100$), corresponding to atoms with thermal velocities ($v\leq 10^3$ m/s) crossing a 1-cm-long cavity.

ACKNOWLEDGMENTS

This work was supported in part by the U.K. Science and Engineering Research Council, the Mexican Consejo Nacional de Ciencia y Tecnologia (CONACyT), the British Overseas Research Scheme, and Marks and Spencer Ltd. through the Weizmann Institute—Imperial College Exchange Scheme, the U.S.A.–Israel Binational Science Foundation, and the Bat-Sheva de Rothschild Foundation.

APPENDIX

The normalization constant P_K for fixed times $t_j=\tau$ and initial coherent state $|\alpha\rangle$ is given by [see Eq. (3.3)]

$$P_K=e^{-\alpha^2}\sum_{n=0}^{\infty}\frac{\alpha^{2n}}{n!}\left[\frac{\cos\Omega_{n+2}\tau}{2}\right]^{2K}. \tag{A1}$$

This series can be summed, using the expansion

$$(\cos\theta)^{2K}=\frac{1}{2^{2K}}\sum_{j=0}^{2K}\frac{2K!}{j!(2K-j)!}e^{2i\theta(K-j)} \tag{A2}$$

and so, with $\theta=\Omega_{n+2}\tau/2$,

$$P_K=\frac{e^{-\alpha^2}}{2^{2K}}\sum_{n=0}^{\infty}\frac{\alpha^{2n}}{n!}\left[\sum_{j=0}^{2K}\frac{2K!}{j!(2K-j)!}e^{2i\theta(K-j)}\right]. \tag{A3}$$

We can now carry out the infinite sum

$$P_K=\frac{(2K!)}{2^{2K}(K!)}+\frac{e^{-\alpha^2}}{2^{2K-1}}\sum_{j=0}^{K-1}\frac{2K!}{j!(2K-j)!}\exp\{\alpha^2\cos[B\tau(K-j)]\}\cos\{\alpha^2\sin[B\tau(K-j)]+(A+2B)\tau(K-j)\}. \tag{A4}$$

We wish to examine the limit of P_K for large K. The most significant terms in the sum (A4) appear to be those for which $j \sim K-1$. The cosine term takes values in the range $(-1,1)$, but the exponential term ensures that only the last few terms in the sum are important if $|\alpha|^2$ is large. Thus we may take only the last term to give

$$P_K = \frac{(2K!)}{2^{2K}(K!)^2}\left[1+2e^{\alpha^2(\cos B\tau-1)}\cos[\alpha^2\sin(B\tau)+(A+2B)\tau]\frac{K}{K+1}\right] . \tag{A5}$$

[1] E. Schrödinger, Naturwissenschaften **23**, 807 (1935); **23**, 823 (1935); **23**, 844 (1935) [English translation by J. D. Trimmer, Proc. Am. Phys. Soc. **124**, 3325 (1980)].

[2] B. Yurke and D. Stoler, Phys. Rev. Lett. **57**, 13 (1986).

[3] W. Schleich, M. Pernigo, and Fam Le Kien, Phys. Rev. A **44**, 2172 (1991); V. Bužek, A. Vidiella-Barranco, and P. L. Knight, Phys. Rev. A **45**, 6570 (1990).

[4] R. Loudon and P. L. Knight, special issue of J. Mod. Opt. **34**, 709 (1987), and other papers in this issue.

[5] J. Opt. Soc. Am. B **4** (10) (1987), special issued edited by H. J. Simble and D. F. Walls.

[6] J. Krause, M. O. Scully, T. Walther, and H. Walther, Phys. Rev. A **39**, 1915 (1989).

[7] G. Rempe, F. Schmidt-Kaler, and H. Walther, Phys. Rev. Lett. **64**, 2783 (1990).

[8] P. Meystre, G. Rempe, and H. Walther, Opt. Lett. **13**, 1078 (1988).

[9] P. Filipowicz, J. Javanainen, and P. Meystre, Phys. Rev. A **34**, 3077 (1986).

[10] C. M. Savage, S. L. Braunstein, and D. F. Walls, Opt. Lett. **15**, 628 (1990).

[11] J. Eiselt and H. Risken, Opt. Commun. **72**, 351 (1989).

[12] P. Meystre, J. J. Slosser, and M. Wilkens, Opt. Commun. **79**, 300 (1990).

[13] J. Gea-Banacloche, Phys. Rev. Lett. **65**, 3385 (1990).

[14] S. J. D. Phoenix and P. L. Knight, Phys. Rev. A **44**, 6023 (1991); V. Bužek, H. Moya-Cessa, P. L. Knight, and S. J. D. Phoenix, *ibid.* **45**, 8190 (1992).

[15] M. Brune, S. Haroche, J. M. Raimond, L. Davidovich, and N. Zagury, Phys. Rev. A **45**, 5193 (1992).

[16] B. Sherman and G. Kurizki, Phys. Rev. A **45**, 7674 (1992).

[17] G. S. Agarwal, M. Orszag, M. O. Scully, and H. Walther (unpublished).

[18] A. Vidiella-Barranco, H. Moya-Cessa, and V. Bužek, J. Mod. Opt. **39**, 1441 (1992).

[19] S. M. Barnett and P. L. Knight, Phys. Rev. A **33**, 2444 (1986); N. Nayak, R. K. Bullough, B. V. Thompson, and G. S. Agarwal, IEEE J. Quantum Electron. **24**, 1331 (1988).

[20] M. O. Scully and W. E. Lamb, Jr., Phys. Rev. **179**, 368 (1969); Ning Lu, Phys. Rev. A **40**, 1707 (1989); J. Janszky and T. Kobayashi, *ibid.* **41**, 4074 (1990); Tran Quang, P. L. Knight, and V. Bužek, *ibid.* **44**, 6092 (1991); S. L. Braunstein, *ibid.* **45**, 6803 (1992).

[21] A. H. Toor and M. S. Zubairy, Phys. Rev. A **45**, 4951 (1992).

[22] M. Brune, J. M. Raimond, and S. Haroche, Phys. Rev. A **35**, 154 (1987).

[23] D. T. Pegg and S. M. Barnett, Phys. Rev. A **39**, 1665 (1989).

[24] D. Meschede, Phys. Rep. **211**, 201 (1992).